Electromagnetic production of Higgs bosons, supersymmetric particles, glueballs, and mesons in ultrarelativistic heavy-ion collisions

Martin Greiner,[1] Mario Vidović,[2,3] and Gerhard Soff[3]
[1] *Department of Physics, University of Arizona, Tucson, Arizona 85721*
[2] *Institut für Theoretische Physik, Johann Wolfgang Goethe-Universität, Postfach 111 932, D-6000 Frankfurt am Main, Germany*
[3] *Gesellschaft für Schwerionenforschung (GSI), Planckstrasse 1, Postfach 110 552, D-6100 Darmstadt, Germany*
(Received 7 December 1992)

The electromagnetic creation of various exotic particles in ultrarelativistic heavy-ion collisions is discussed. The production of intermediate mass Higgs bosons of the minimal supersymmetric extension of the standard model is enhanced over the standard model Higgs boson formation for certain model parameter choices and as a consequence might be detectable at the CERN Large Hadron Collider and Superconducting Super Collider. We also investigate the electromagnetic generation of supersymmetric fermions and bosons as well as glueballs, mesons, and fermions.

PACS number(s): 25.75.+r, 23.20.−g

I. INTRODUCTION

Ultrarelativistic heavy-ion collisions represent an important tool to investigate such frontier topics as, for example, the possible formation of a quark-gluon plasma. Furthermore, a broad spectrum of new exotic particles could be generated, which usually is the realm of the e^+e^- or pp collider.

In central ultrarelativistic heavy-ion collisions new particles can be created in single-particle encounters of the individual constituents. A simple geometrical estimate yields that the number of independent nucleon-nucleon collisions in a heavy-ion collision should scale roughly with $A^{4/3}$, where A nucleons of the projectile collide with a certain number of target nucleons, which should be proportional to the nuclear thickness $A^{1/3}$. For a Pb+Pb collision this corresponds to about 1200–1500 independent nucleon-nucleon collisions. As a consequence of this simple incoherent picture particle production cross sections in heavy-ion collisions are by about 3 orders of magnitude larger than in pp collisions [1]. On the other hand, the c.m. energy per nucleon is expected to be about 2.5 times larger for the pp mode at the planned ultrarelativistic hadron collider LHC (Large Hadron Collider) at CERN and SSC (Superconducting Super Collider) in Texas and, even more important, the luminosity for the pp mode is expected to be 5 orders of magnitude larger than for the heavy-ion option. As a consequence, the particle production rates in ultrarelativistic heavy-ion collisions will be suppressed by typically 2 orders of magnitude with respect to pp collisions.

The nuclear velocities are nearly equal to the speed of light, so that in view of the high charge number Z electromagnetic particle production will be possible via the strong transverse electromagnetic fields. A rough estimate leads to a maximum frequency $\omega_{\max} = 1/t_{\text{coll}} = \gamma/R$ contained in the electromagnetic field. $\gamma = (1 - v^2)^{-1/2}$ is the Lorentz contraction factor and R is the nuclear radius. For the proposed LHC with $E_{\text{ion}} = 3.5$ TeV/nucleon ($\gamma \approx 3500$) and SSC with 8 TeV/nucleon ($\gamma \approx 8000$) in a Pb+Pb collision this leads to $\omega_{\max} \approx 100$ GeV (LHC) and $\omega_{\max} \approx 250$ GeV (SSC). This mass regime exceeds the one which can be reached at the existing e^+e^- collider. As for an e^+e^- collider the electromagnetic production mechanism at a heavy-ion collider would be relatively clean. As a consequence, the electromagnetic production of exotic particles with masses exceeding the e^+e^--collider regime in ultrarelativistic heavy-ion collisions might be a promising alternative.

In a previous publication [2] we outlined the theoretical concept for the electromagnetic particle production in ultrarelativistic heavy-ion collisions. Starting from quantum electrodynamics Feynman diagrams we derived the production cross section within the framework of the Weizsäcker-Williams method. It has been demonstrated [2] that the transverse momentum components of the virtual photons are suppressed by the Lorentz contraction factor γ compared with their longitudinal momentum component and energy. As a by-product we also derived an impact-parameter dependent differential cross section. This differential cross section splits up into a scalar and pseudoscalar contribution; for the scalar part the electromagnetic fields of the colliding heavy ions have to be parallel whereas for the pseudoscalar part the electromagnetic fields have to be perpendicular. The interplay of these two different mechanisms leads to some neat consequences for the electromagnetic production of a single neutral boson, a pair of charged bosons, and a pair of charged fermions.

In this publication we apply the formalism for the electromagnetic particle production to specific exotic particles. In Sec. II we focus on the electromagnetic production of Higgs bosons as required from the minimal supersymmetric extension of the standard model; the standard

model Higgs boson has been dealt with before [3–14]. In Sec. III we reconsider the electromagnetic production of supersymmetric particles. Electromagnetic production of various mesons is the subject of Sec. IV; we discuss scalar and pseudoscalar mesons, glueball candidates, and pairs of charged mesons. For completeness we also mention the electromagnetic production of leptons in Sec. V. Our conclusions are presented in Sec. VI.

In an earlier publication [2] we demonstrated very extensively, how to derive the equivalent photon cross section from Feynman diagrams directly. In lowest, i.e., second, order the electromagnetic potentials of the two colliding heavy ions enter into the S-matrix element; the heavy ions A_1 and A_2 are assumed to move with opposite constant velocities on straight trajectories, which are separated by the impact parameter **b**. The electromagnetic potentials couple to a transition current depending on the outgoing particles X to be produced. Of course, this coupling is gauge invariant, so that the transition current is conserved. It is this conservation together with the illustrative assumption that, for the considered ultrarelativistic heavy-ion collision energies, the transverse momentum components of the incoming virtual photons are suppressed over their longitudinal components by the Lorentz contraction factor γ, which help to make the identification with the equivalent photons. The cross section, which is an integration of the squared S-matrix element over the phase space of the outgoing produced particles and the impact parameter, is presented in Eq. (31) of Ref. [2].

Small impact parameters have to be excluded for the sake of a trigger on peripheral collisions of the heavy ions and in order to discard the accompanying large hadronic background for the particle detection. This motivates the introduction of a sharp cutoff impact parameter $b_c = 2R$, where R is the nuclear radius and which leads to a reduced total cross section

$$\sigma^{\rm red}_{A_1A_2\to A_1A_2X} = \int_0^\infty db\,\frac{d\sigma_{A_1A_2\to A_1A_2X}}{db}\,\Theta(b-2R) = \int_0^\infty db\,2\pi b\,\frac{d^2\sigma_{A_1A_2\to A_1A_2X}}{db^2}\,\Theta(b-2R) \quad . \tag{1}$$

We define the quantity $\sigma^{\rm red}_{A_1A_2\to A_1A_2X}/\sigma_{A_1A_2\to A_1A_2X}$ as a reduction factor.

The polarized two-photon fusion cross sections which we will use in the following discussions are indicated in Eqs. (48)–(51) of Ref. [2]. For a neutral scalar boson (b_s) with spin J, the pseudoscalar two-photon fusion cross section vanishes and the scalar one has the structure

$$\sigma^s_{\gamma\gamma\to b_s}(\omega_1,\omega_2) = 2(2J+1)\frac{8\pi^2}{m_{b_s}}\,\Gamma_{b_s\to\gamma\gamma} \times\delta(4\omega_1\omega_2 - m^2_{b_s}) \quad , \tag{2}$$

m_{b_s} is the boson mass and $\Gamma_{b_s\to\gamma\gamma}$ denotes the two-photon decay width of the boson. $J = 0$ for a spin-0 boson and $J = 2$ for a spin-2 boson; a spin-1 boson cannot be produced via two real photons [15]. For a neutral pseudoscalar boson ($b_{\rm ps}$) the scalar two-photon fusion cross section vanishes and the pseudoscalar one has the same structure as in Eq. (2). For a nuclear charge form factor we used the one for a homogeneously charged sphere.

II. ELECTROMAGNETIC PRODUCTION OF INTERMEDIATE MASS HIGGS BOSONS OF THE MINIMAL SUPERSYMMETRIC EXTENSION OF THE STANDARD MODEL

The electromagnetic production of the intermediate mass standard model (SM) Higgs boson in ultrarelativistic heavy-ion collisions has been discussed extensively [3–14]. It was argued that the SM Higgs boson detection in the intermediate mass regime, i.e., $m_Z < m_H < 2m_W$, would be accessible for the planned ultrarelativistic heavy-ion collider at LHC and SSC with the help of the relatively clean electromagnetic production mechanism. Total and reduced cross sections have been determined within the equivalent photon method. The reduced cross sections of several tens (LHC) and some hundreds (SSC) of pb turned out to be about 40 times larger than the hadroproduction cross sections for pp collisions. But contrary to this, the expected luminosity of 10^{28} cm^{-2} sec^{-1} for the LHC and SSC heavy-ion collider is about 5 orders of magnitude lower than the one for the suggested pp-collider modes at LHC and SSC. With a running time of 10^7 sec/yr ($\approx 1/3$ yr) this leads to about 48 (6) produced SM Higgs bosons with an assumed mass of 100 GeV at SSC (LHC). These numbers are discouraging because they do not allow for a detection of the SM Higgs boson via rare decay modes such as the two-photon decay or the decay into four leptons, which have branching ratios of about 10^{-3}. The dominant $b\bar{b}$ decay mode disappears in the background, which consists of directly produced $b\bar{b}$ pairs.

What is the situation in more elaborated models for the spontaneous symmetry breaking mechanism? For example, in the minimal supersymmetric extension of the standard model (MSSM) [16] two Higgs doublet fields are required, which result in two scalar, one pseudoscalar, and a pair of charged Higgs bosons. Besides the unknown parameters stemming from the supersymmetric (SUSY) sector, two additional free parameters enter in this model, which we will choose as in Ref. [16] to be the ratio $\tan\beta$ of the two vacuum expectation values of the two Higgs doublet fields and the mass $m_{H^\pm}$ of the charged Higgs boson. In certain regions of this parameter space it may be that the two-photon minimal supersymmetric standard model (MSSM) Higgs production is enhanced over the corresponding SM Higgs production; if this enhancement turns out to be large enough it might become feasible to detect the MSSM Higgs bosons via their rare decays (two-photon decay, four-lepton decay). As an alternative it might also be possible to detect the MSSM Higgs bosons via their dominant $b\bar{b}$ decay; because of their enhanced production more Higgs decays into a $b\bar{b}$ pair will take place, whereas the rate of the directly produced $b\bar{b}$

pairs will not be affected by the various new model parameters, so that the former might be distinguishable as a small peak in the invariant mass spectrum of the latter. Of course there are also other regions in the parameter space where there will be a suppression instead of an enhancement in the two-photon MSSM Higgs production mechanism. The following discussion is intended to clarify whether there are regions in the MSSM parameter space which allow for a clear Higgs boson detection in peripheral ultrarelativistic heavy-ion collisions.

We will only concentrate on the two scalar (H_{s1}, H_{s2}) and the pseudoscalar ($H_{\rm ps}$) MSSM Higgs bosons. At tree level their masses depend only on the two parameters $\tan\beta$ and $m_{H^\pm}$ [16]:

$$m^2_{H_{\rm ps}} = m^2_{H^\pm} - m^2_W,$$
$$m^2_{H_{s1,s2}} = \frac{1}{2}\left[m^2_{H_{\rm ps}} + m^2_Z \pm \sqrt{(m^2_{H_{\rm ps}} + m^2_Z)^2 - 4m^2_{H_{\rm ps}} m^2_Z \cos^2(2\beta)}\right] , \tag{3}$$

m_Z and m_W are the mass of the Z and W bosons, respectively. These mass relations lead to the remarkable predictions

$$m_{H^\pm} \geq m_W, \quad m_{H_{s1}} \geq m_Z, \quad \text{and} \quad m_{H_{s2}} \leq m_Z \quad . \tag{4}$$

This implies that a low mass scalar Higgs boson should exist which does not exceed the mass of the Z boson. If one-loop corrections are incorporated, the mass relations in Eq. (3) and the tree-level mixing angle

$$\tan 2\alpha = \frac{m^2_{H_{\rm ps}} + m^2_Z}{m^2_{H_{\rm ps}} - m^2_Z} \quad , \tag{5}$$

which arises in the process of diagonalizing the 2×2 neutral scalar Higgs mass matrix, have to be modified [17–22]. With increasing mass of the top quark, these modifications are not negligible, but still not drastic. For example, the upper limit on the mass of the light scalar Higgs boson might be pushed by a few tens of GeV into the intermediate mass regime. As a first estimate for the production and detectability of the MSSM Higgs bosons in comparison to the SM Higgs boson in ultrarelativistic heavy-ion collisions we will neglect radiative corrections.

The elementary two-photon fusion cross section $\sigma_{\gamma\gamma\to H}$ is given by Eq. (2) with $J = 0$ and enters in the Higgs production cross section (33) of Ref. [2] and in (1). The physical nature of the MSSM Higgs bosons enters in the two-photon decay width; it is given by the expression

$$\Gamma_{H\to\gamma\gamma} = \frac{\alpha^2 G_F}{128\pi^3} m^3_H \left|\sum_i I^i_H\right|^2 \quad , \tag{6}$$

where α is the fine structure constant, $G_F/(\hbar c)^3 = 1.166\,37 \times 10^{-5}$ GeV^{-2} is the Fermi coupling constant, m_H is the mass of the Higgs boson, and the subscript H stands for H_{s1}, H_{s2}, $H_{\rm ps}$, or $H_{\rm SM}$, respectively. For the MSSM Higgs bosons H_{s1}, H_{s2}, and $H_{\rm ps}$, all fermions, W bosons, charged Higgs bosons, sfermions, and charginos contribute to the loop amplitudes I^i_H, which can be deduced from Ref. [16]. Observe the misprint in the sfermion-loop amplitude published in Ref. [16], which has to be multiplied with the factor $m^2_Z/m^2_{\tilde f}$, where $m_{\tilde f}$ represents the sfermion mass. For the coupling factor $R^H_{\tilde\chi^\pm}$ in the chargino amplitude $I^{\tilde\chi^\pm_j}_H$ we used the expression [23]

$$R^{H_{s1}}_{\tilde\chi^\pm_j} = \frac{2}{\sin\beta}\left[\frac{m_{\tilde\chi^\pm_j}}{m_W}\frac{\sin\alpha}{2} + Q_{jj}\sin(\beta-\alpha) - R_{jj}\sin\alpha\right],$$
$$R^{H_{s2}}_{\tilde\chi^\pm_j} = \frac{2}{\sin\beta}\left[\frac{m_{\tilde\chi^\pm_j}}{m_W}\frac{\cos\alpha}{2} - Q_{jj}\cos(\beta-\alpha) - R_{jj}\cos\alpha\right], \tag{7}$$
$$R^{H_{\rm ps}}_{\tilde\chi^\pm_j} = -\frac{2}{\sin\beta}\left[\frac{m_{\tilde\chi^\pm_j}}{m_W}\frac{\cos\beta}{2} - Q_{jj}\cos 2\beta - R_{jj}\cos\beta\right]$$

with

$$Q_{jj} = \frac{1}{\sqrt{2}}U_{j2}V_{j1}, R_{jj} = \frac{1}{2m_W}(M_{\rm SU(2)}U_{j1}V_{j1} + \mu U_{j2}V_{j2})$$

instead of the misleading expression in Ref. [16]. $M_{\rm SU(2)}$ and μ represent as free parameters the SU(2) gaugino mass and a parameter for the mixing of the two Higgs doublet fields in the superpotential, respectively. The two chargino masses $m_{\tilde\chi^\pm_j}$ and the unitary matrices U_{ij} and V_{ij} needed for the diagonalization of the chargino mass matrix depend on $M_{\rm SU(2)}$, μ, and $\tan\beta$. They are given, for example, in Ref. [24]. In addition to the indicated free parameters the mass of the top quark and of the sfermions (sleptons and squarks) also enter as free parameters in the two-photon decay width (6) of the MSSM Higgs bosons. For comparisons we also need to consider the two-photon decay width of the SM Higgs boson $H_{\rm SM}$. It has the same structure as in Eq. (6), but here only the W boson and the fermions contribute to the loop amplitudes $I^i_{H_{\rm SM}}$. An explicit expression for $\Gamma_{H_{\rm SM}\to\gamma\gamma}$ can be taken from Ref. [25].

In our numerical calculations we fixed the mass of the top quark equal to $m_t = 150$ GeV. The masses of the sfermions have been assumed to be identical and have been chosen to be $m_{\rm sfe} = 200$ GeV. A variation towards a higher mass of this rather low value only has a minor impact on the two-photon decay width of the H_{s1} and H_{s2} Higgs bosons and no influence on the two-photon decay width of $H_{\rm ps}$. The remaining free parameters $\tan\beta$,

$m_{H^\pm}$, $M_{SU(2)}$, and μ have been varied.

A heavy particle such as the Higgs boson will be created in the vicinity of high electromagnetic field densities appearing in ultrarelativistic heavy-ion collisions. This will occur predominantly at rather small impact parameters, which for the sake of a clean experimental detection signal have to be excluded. Therefore we introduce a small impact-parameter cutoff in the production cross section as in Eq. (1) and first consider this reduced production cross section relative to the total equivalent photon cross section (31) of Ref. [2]. Observe that this reduction factor only depends on the mass, the overall nature of the Higgs boson, i.e., scalar or pseudoscalar, and the c.m. energy of the heavy ions; the model dependence via the two-photon decay width drops out. Figure 3 in [2] depicts the reduction factor for a scalar and pseudoscalar Higgs boson; only LHC ($\gamma = 3500$) and SSC ($\gamma = 8000$) energies have been considered for the heavy-ion collisions. As expected, the reduction factor decreases with increasing Higgs boson mass and increases with increasing collider energy; it is also nearly the same for a scalar or pseudoscalar boson. For a mass of $m_H = 100$ GeV and for LHC (SSC) energies the reduction factor for a scalar Higgs amounts to $\sigma^{\rm red}/\sigma^{\rm WW} = 0.49$ (0.67) and for a pseudoscalar Higgs $\sigma^{\rm red}/\sigma^{\rm WW} = 0.50$ (0.71).

For the SM Higgs production in ultrarelativistic heavy-ion collisions these results have some far reaching consequences. The reduced cross section (1) for the SM Higgs production in a Pb+Pb collision is shown in Fig. 1. For Higgs masses in the intermediate mass regime, i.e., $m_Z \le m_H \le 2m_W$, the reduced production cross section is several tens of pb for LHC energies and some hundreds of pb for SSC energies. For the dominant decay mode of a SM Higgs boson into a $b\bar{b}$ quark pair the rates are too low to identify them from the invariant mass spectrum of the directly produced $b\bar{b}$ pairs [14]. Evidently these production rates are also too low for the detection via rare SM Higgs decay modes as, for example, the two-photon or four-lepton decay, which exhibit typical branching ratios of about 10^{-3}. Thus it appears that a SM Higgs search in the intermediate mass regime is not a feasible experiment in ultrarelativistic heavy-ion collisions at LHC and SSC.

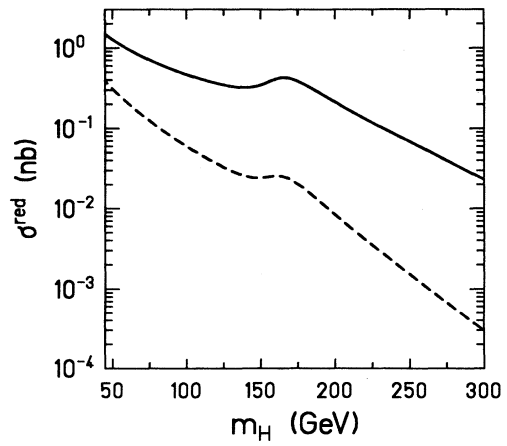

FIG. 1. Reduced production cross section depending on the $H_{\rm SM}$ mass in a Pb+Pb collision at LHC (dashed line) and SSC energies (solid line).

The production cross sections of the MSSM Higgs bosons H_{s1}, H_{s2}, $H_{\rm ps}$ and the one of the SM Higgs boson $H_{\rm SM}$ incorporate a different two-photon decay width. As a consequence the ratio of the MSSM Higgs production cross section with respect to the SM Higgs production cross section, both considered for the same Higgs mass, is given by the corresponding ratio of the two-photon decay widths:

$$\frac{\sigma^{\rm red}_{\rm Pb+Pb\to Pb+Pb+H_{MSSM}}}{\sigma^{\rm red}_{\rm Pb+Pb\to Pb+Pb+H_{SM}}} = \frac{\Gamma_{H_{\rm MSSM}\to\gamma\gamma}}{\Gamma_{H_{\rm SM}\to\gamma\gamma}} \quad . \tag{8}$$

This ratio is depicted for H_{s1} in Fig. 2 and for $H_{\rm ps}$ in Fig. 3. We do not present a figure for H_{s2} because, according to the tree-level mass relations (3), its mass cannot be in the intermediate mass regime, although to some extent radiative corrections might push its mass into this regime for certain choices of the free MSSM parameters.

Various choices of the free parameters $\tan\beta$ and $M_{SU(2)}$ are considered for the ratio (8), which also depends on $m_{H^\pm}$ and μ. The chosen values of $\tan\beta$ and $M_{SU(2)}$ are consistent with present experimental limits, whereas the region -50 GeV $\le \mu \le 100$ GeV has to be excluded [26]. According to the mass relations (3) the mass of H_{s1} depends on $M_{H^\pm}$ and $\tan\beta$, whereas $m_{H_{\rm ps}}$ only depends on $m_{H^\pm}$. The intermediate mass regime $m_Z \approx 90$ GeV $\le m_H \le 2m_W \approx 160$ GeV corresponds to $m_W \approx 80$ GeV $\le m_{H^\pm} \le 160 - 180$ GeV for H_{s1}, where the exact upper bound depends slightly on $\tan\beta$, and to 120 GeV $\le m_{H^\pm} \le 180$ GeV for $H_{\rm ps}$. As demon-

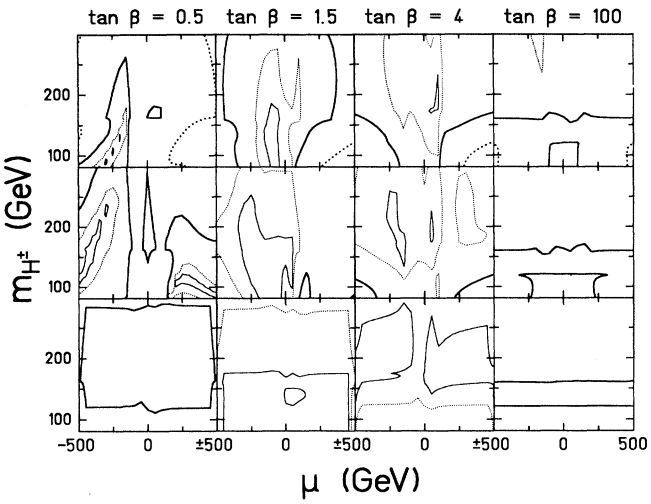

FIG. 2. The ratio $\Gamma_{H_{s1}\to\gamma\gamma}/\Gamma_{H_{\rm SM}\to\gamma\gamma}$ is shown depending on $m_{H^\pm}$ and μ and various values of $\tan\beta$ and $M_{SU(2)}$. Each column corresponds to an indicated value of $\tan\beta$ and each row corresponds from top to bottom to $M_{SU(2)} = 50$ GeV, 100 GeV, and 500 GeV. The contour lines thin solid, thin dotted, thick solid, and thick dotted represent $\Gamma_{H_{s1}\to\gamma\gamma}/\Gamma_{H_{\rm SM}\to\gamma\gamma} = 0.01$, 0.1, 1, and 10, respectively.

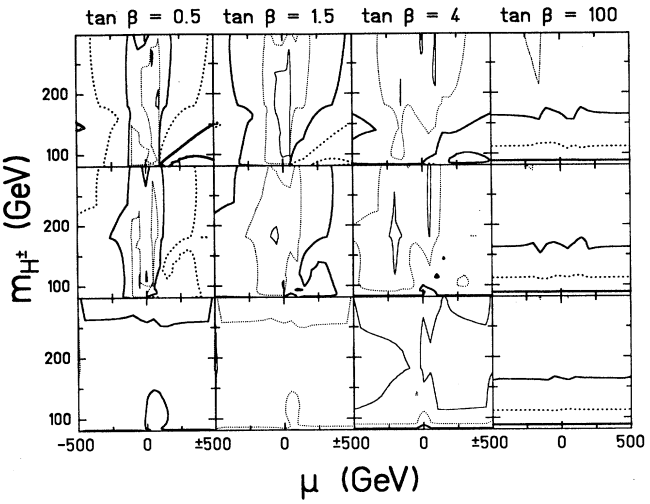

FIG. 3. The ratio $\Gamma_{H_{ps}\to\gamma\gamma}/\Gamma_{H_{SM}\to\gamma\gamma}$ is shown depending on $m_{H^\pm}$ and μ and various values of $\tan\beta$ and $M_{SU(2)}$. Each column corresponds to an indicated value of $\tan\beta$ and each row corresponds from top to bottom to $M_{SU(2)} = 50$ GeV, 100 GeV, and 500 GeV. The contour lines thin solid, thin dotted, thick solid, thick dotted, and very thick solid represent $\Gamma_{H_{ps}\to\gamma\gamma}/\Gamma_{H_{SM}\to\gamma\gamma} = 0.01$, 0.1, 1, 10, and 100, respectively.

strated in Figs. 2 and 3 the ratio $\Gamma_{H_{MSSM}\to\gamma\gamma}/\Gamma_{H_{SM}\to\gamma\gamma}$ depends sensitively on the chosen parameters. It can vary from rather small values of about 0.01 to even such a large value of 100. The depicted contour lines thin solid, thin dotted, thick solid, thick dotted, and very thick solid represent $\Gamma_{H_{MSSM}\to\gamma\gamma}/\Gamma_{H_{SM}\to\gamma\gamma} = 0.01$, 0.1, 1, 10, and 100, respectively. First we focus on the intermediate mass regime of the heavy scalar Higgs boson H_{s1}. Interesting parameter regions are those where $\Gamma_{H_{s1}\to\gamma\gamma}$ becomes nearly ten times larger than $\Gamma_{H_{SM}\to\gamma\gamma}$ or more. This dominantly occurs for large-μ values with a very low SU(2) gaugino mass of $M_{SU(2)} \approx 50$ GeV and all choices of $\tan\beta$; however, for such a rather low value of $M_{SU(2)}$ the mass of the lighter chargino approaches close to its present experimental limit of $m_{\tilde{\chi}^\pm} \geq 45$ GeV [27]. Other parameter regions for $\Gamma_{H_{s1}\to\gamma\gamma}/\Gamma_{H_{SM}\to\gamma\gamma}$ lead to values which are to some extent drastically smaller than 1. The intermediate mass pseudoscalar MSSM Higgs boson H_{ps} possesses a broader parameter region of interest. Again for $M_{SU(2)} \approx 50$ GeV and for all values of $\tan\beta$ the ratio $\Gamma_{H_{ps}\to\gamma\gamma}/\Gamma_{H_{SM}\to\gamma\gamma}$ might become larger than 10 for large absolute values μ; note that for the extreme choice $\tan\beta = 0.5$ the two-photon decay width $\Gamma_{H_{ps}\to\gamma\gamma}$ might even become 100 times larger than the SM Higgs two-photon decay width $\Gamma_{H_{SM}\to\gamma\gamma}$ for large values of μ. Also, the extreme choices $\tan\beta = 100$ with all chosen values of $M_{SU(2)}$ and $\tan\beta = 0.5$ with $M_{SU(2)} = 100$ GeV lead to $\Gamma_{H_{ps}\to\gamma\gamma}/\Gamma_{H_{SM}\to\gamma\gamma}$ ratios in the vicinity of 10.

To summarize, parameter regions, where $M_{SU(2)} = 50$ GeV has a rather low value or where $\tan\beta = 100$ takes on an extreme value, lead to an enhancement of the two-photon decay width $\Gamma_{H_{s1}\to\gamma\gamma}$ and $\Gamma_{H_{ps}\to\gamma\gamma}$ over the two-photon decay width $\Gamma_{H_{SM}\to\gamma\gamma}$ of the SM Higgs boson in the intermediate mass regime; in these cases the enhancement can even exceed a factor of 10. It would be interesting to know to what extent radiative corrections could modify this insight.

Figure 1 shows reduced cross sections for the SM Higgs production at LHC and SSC energies, which have to be multiplied with the ratio (8) depicted in Figs. 2 and 3 in order to deduce the cross sections for the H_{s1} and H_{ps} production. As demonstrated in Fig. 3 in [2] the reduction factors for a scalar and pseudoscalar boson are nearly the same. The stated reduced cross sections scale with the ratio $\Gamma_{H_{MSSM}\to\gamma\gamma}/\Gamma_{H_{SM}\to\gamma\gamma}$ with respect to the reduced SM Higgs boson cross section; confer again Eq. (8). The ratio of the two two-photon decay widths may roughly vary from 10 to 10^{-2} over the chosen range of free parameters. The case of enhanced production cross sections for H_{s1} and H_{ps} also leads to enhanced production rates. With the expected collider performance discussed before and an enhancement factor of 10, about 480 (60) produced MSSM Higgs bosons H_{s1} and H_{ps} with an assumed mass of $m_H = 100$ GeV and about 340 (20) H_{s1} and H_{ps} Higgs bosons with $m_H = 150$ GeV are to be expected for SSC (LHC) per year; again this enhancement is only to be expected for rather low choices of the SU(2) gaugino mass or, in addition for H_{ps}, for the extreme choices of very large or low values of the parameter $\tan\beta$.

Even for these optimistic parameter regimes the enhanced production rates for the heavy scalar (H_{s1}) and the pseudoscalar (H_{ps}) MSSM Higgs bosons having intermediate masses do not suffice to allow for their detection via the rare decay modes $H \to \gamma\gamma$ or $H \to l^+l^-l^+l^-$ which still have branching ratios of about 10^{-3} or less [22,28]. On the other hand the dominant decay mode into a $b\bar{b}$ pair for an intermediate mass Higgs boson might become of interest again for H_{s1} and H_{ps}: The enhancement factor of about 10 in the optimistic MSSM parameter regime leads to signal rates which are enhanced by the same factor. In contrast to this, the background stemming from directly produced $b\bar{b}$ pairs via two-photon fusion stays exactly the same as in the H_{SM} case. As a consequence the signal $b\bar{b}$ pairs are enhanced with respect to the background $b\bar{b}$ pairs, so that it might be feasible to detect the intermediate mass H_{s1} and H_{ps} as a small peak in the invariant $b\bar{b}$ mass spectrum.

III. ELECTROMAGNETIC PRODUCTION OF SUSY PARTICLES

In two recent publications [5,29] the electromagnetic production of supersymmetric (SUSY) particles in ultrarelativistic heavy-ion collisions has been proposed and discussed within the framework of the equivalent photon method. In Ref. [29] only total production cross sections are considered. An impact-parameter cutoff according to Eq. (1) has not been taken into account. The presented derivation of an impact-parameter dependent generalization of the equivalent photon method was incomplete; the underlying assumption that the transverse momenta

of the virtual photons do not contribute to the invariant matrix element does not hold. This formulation has been modified and corrected in Ref. [2].

The supersymmetric partners of the leptons and quarks, which are called sleptons and squarks, have the same charge as their standard model counterparts, but have spin 0 and thus represent bosons. Similiarly, winos and higgsinos have the same charge as their counterparts, which are the W boson and a possible charged Higgs boson, but exhibit spin 1/2 and therefore represent fermions. The coupling of these exotic charged particles are fixed to lowest, i.e., second, order in two-photon collisions, so that actually their production rates will be model independent and depend only on the mass and the heavy-ion collision energy; confer Eqs. (48)–(51) in [2]. The masses of the supersymmetric particles will lie above 20–50 GeV [27]. The reduction factor due to the cutoff of small impact parameters results to be $R = \sigma^{\rm red}_{\rm Pb+Pb\to Pb+Pb+b^+b^-}/\sigma_{\rm Pb+Pb\to Pb+Pb+b^+b^-} = 0.43\,(0.61)$ for a boson mass of $m_{b^\pm} = 50$ GeV, $R = 0.29\,(0.46)$ for a boson mass of $m_{b^\pm} = 100$ GeV, and $R = 0.17\,(0.32)$ for a boson mass of $m_{b^\pm} = 200$ GeV at LHC (SSC) energies. For fermions with mass $m_{f^\pm} = 50$, 100, and 200 GeV we find $\sigma^{\rm red}_{\rm Pb+Pb\to Pb+Pb+f^+f^-}/\sigma_{\rm Pb+Pb\to Pb+Pb+f^+f^-} = 0.41\,(0.61)$, $0.24\,(0.45)$, and $0.10\,(0.28)$ at LHC (SSC) energies, respectively. In Fig. 4 we display the reduced production cross sections of heavy charged bosons and fermions in the mass range 50–200 GeV in ultrarelativistic Pb+Pb collisions at LHC and SSC energies. For the radius of the Pb nucleus we used $R = 7.1$ fm. The production cross sections for fermions are larger than those for bosons. For a fermion mass $m_{f^\pm} = 50$, 100, and 200 GeV we find reduced cross sections of $\sigma^{\rm red}_{\rm Pb+Pb\to Pb+Pb+f^+f^-} = 3.44\,(45.1)$, $0.0256\,(1.43)$, and $0.22\times10^{-4}\,(1.5\times10^{-2})$ nb at LHC (SSC) energies; for a boson mass $m_{b^\pm} = 50$, 100, and 200 GeV $\sigma^{\rm red}_{\rm Pb+Pb\to Pb+Pb+b^+b^-} = 0.74\,(8.27)$, $0.72\times10^{-2}\,(0.30)$, and $0.97\times10^{-5}\,(0.39\times10^{-2})$ nb. These results are about a factor of 1.5 higher than the ones obtained in Ref. [5]. The difference traces back to the simplified equivalent photon distribution used in the latter reference and the neglect of polarized two photon fusion cross sections.

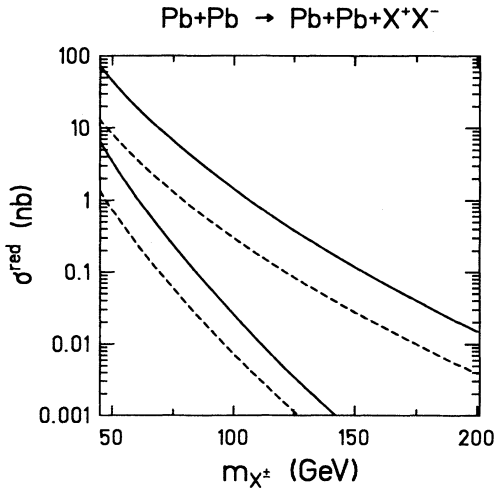

FIG. 4. Reduced production cross sections of heavy (spin-0) bosons (dashed lines) and fermions (solid lines) in ultrarelativistic Pb+Pb collisions at LHC (lower curves) and SSC (upper curves) energies.

For an expected LHC luminosity of 10^{28} cm^{-2} sec^{-1} and a running time of 10^7 sec/yr this implies that about 356 and 2 fermions with mass $m_{f^\pm} = 50$ and 100 GeV and about 76 charged (spin-0) bosons with mass $m_{b^\pm} = 50$ GeV could be generated at LHC. About 4674, 148, and 1 fermions with mass $m_{f^\pm} = 50$, 100, and 200 GeV and about 857 and 31 charged (spin-0) bosons with mass $m_{b^\pm} = 50$ and 100 GeV could be produced per year at the SSC.

For not too high masses of the charged supersymmetric particles the production rates seem to be sufficient; once a supersymmetric particle is produced it can only decay into an odd number of SUSY particles. At the end of the decay cascade an odd number of the lightest supersymmetric particles evolve, which can hardly be detected. Therefore, in principle, one would always trigger on missing energy and momentum events together with a multiplicity of lepton and quark-jet events. A full acceptance detector would be needed for such an investigation.

IV. ELECTROMAGNETIC PRODUCTION OF MESONS

A. Scalar and pseudoscalar mesons

In peripheral heavy-ion collisions also scalar and pseudoscalar mesons as, for example, π^0, η, η', can be created electromagnetically. This allows for QCD studies; electromagnetic form factors, two-photon decay widths, and decay modes of the mesons could be deduced. Since the photons become quasireal in ultrarelativistic heavy-ion collisions, the generated mesons can only be either of spin 0 or of spin 2; the production of a spin-1 meson through two real photons is forbidden kinematically [15]. Furthermore, the final state needs to be a meson with charge conjugation quantum number $C = +1$.

Final state interactions have been neglected in our calculations for meson formation. Thus the description of the electromagnetic meson production in heavy-ion collisions is given by Eqs. (1) and (2). The two-photon decay width entering in Eq. (2) is taken from experimental data [27,30–32].

Let us focus on the π^0 production first, which is the lightest of the known mesons. The experimental two-photon decay width of the pion amounts to $\Gamma_{\pi^0\to\gamma\gamma} = 7.7 \pm 0.6$ eV. Because of the relatively low mass of $m_{\pi^0} = 134.97$ MeV most of the pions will be produced outside the central collison region ($b < 2R$) for the considered energies at SSC ($\gamma = 8000$), LHC ($\gamma = 3500$), and the Brookhaven Relativistic Heavy Ion Collider (RHIC) ($\gamma = 100$). This is demonstrated in Fig. 5, where the normalized differential cross section $\frac{1}{\sigma^{\rm tot}}\frac{d\sigma}{db}$ is plotted for the π^0 production in Pb+Pb collisions. As a consequence

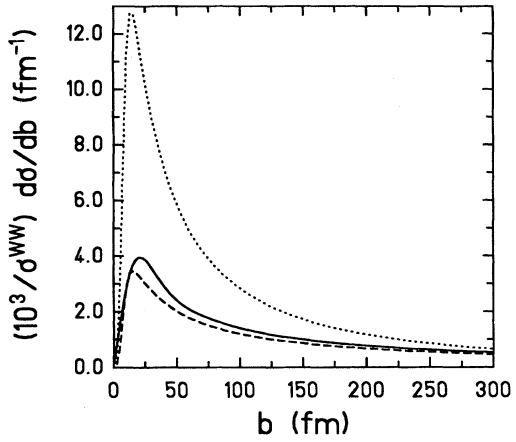

FIG. 5. Normalized impact-parameter dependent Weizsäcker-Williams cross section for the π^0 production. The dotted, solid, and dashed curves represent Lorentz contraction factors of $\gamma = 100$ (RHIC), $\gamma = 3500$ (LHC), and $\gamma = 8000$ (SSC) in a Pb+Pb collision. For the nuclei the form factor of a homogeneously charged sphere has been applied.

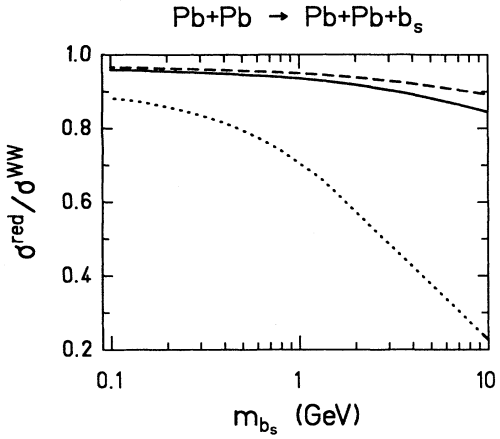

FIG. 6. Reduction factors $\sigma^{\rm red}/\sigma^{\rm WW}$ in dependence on the scalar boson mass for RHIC ($\gamma = 100$, dotted line), LHC ($\gamma = 3500$, solid line), and SSC ($\gamma = 8000$, dashed line) Pb+Pb collision energies.

the reduced cross section (1) and the total Weizsäcker-Williams cross section will be nearly the same. For Pb+Pb collisions at RHIC energies ($\gamma = 100$) we calculated $\sigma^{\rm WW} = 5.92 \pm 0.46$ mb and $\sigma^{\rm red} = 5.38$ mb, for LHC energies ($\gamma = 3500$) $\sigma^{\rm WW} = 40.3 \pm 3.1$ mb and $\sigma^{\rm red} = 39.1$ mb, and for SSC energies ($\gamma = 8000$) $\sigma^{\rm WW} = 54.9 \pm 4.3$ mb and $\sigma^{\rm red} = 53.6$ mb. The reduction of the total cross section due to the central impact-parameter cutoff has no dramatic consequences; it is of the same order of magnitude as the variation originating from the experimental uncertainty of the two-photon decay width.

For mesons with masses well above the pion mass similar conclusions hold. The reduction factors of the Weizsäcker-Williams cross sections stay close to one for LHC and SSC heavy-ion collision energies. But for RHIC energies the reduction factors drop tremendously as soon as the meson mass exceeds a few hundred MeV; this is exemplified in Fig. 6 for scalar mesons. Nearly identical results hold for pseudoscalar mesons. The reason for this traces back to the low maximum frequency $\omega_{\rm max} = \gamma/R \approx 3$ GeV contained in the electromagnetic fields of a Pb nucleus moving with RHIC energies ($\gamma = 100$), so that mesons with a mass of about 1 GeV can only be produced in the vicinity of the strongest electromagnetic field densities, which occur at small impact parameters and therefore drop out by the impact-parameter cutoff. This demonstrates the necessity of the reduction factor for this energy and mass region. In Table I we summarize the reduced production cross sections of various mesons. Roughly spoken, the reduced production cross sections are in the range from 0.1 mb to several tens of mb for the mesons, depending of course strongly on the heavy-ion collision energy and detailed aspects such as meson mass and two-photon decay width.

B. Glueballs

One prediction of QCD is the existence of exotic bound states containing several gluons and quarks. Bound states, which predominantly contain gluons compared to quarks, are called glueballs. A definite experimental evidence for their existence has not been provided, but the general point of view is that glueballs should be produced in reactions involving J/ψ decays. Several theoretical models are used as an approximation of the solution of the QCD equations of motion to predict the properties of

TABLE I. Cross sections of various scalar and pseudoscalar mesons.

				$\sigma^{\rm red}$ ($\sigma^{\rm WW}$) (mb)		
Particle	$J^{\rm PC}$	mass (MeV)	$\Gamma_{\gamma\gamma}$ (keV)	$\gamma = 100$	$\gamma = 3500$	$\gamma = 8000$
π^0	0^{-+}	134.97	0.0077	5.38 (5.92)	39.1 (40.3)	53.6 (54.9)
η	0^{-+}	547.45	0.51	1.45 (1.75)	22.9 (23.8)	33.8 (34.9)
$\eta'(958)$	0^{-+}	957.75	4.5	1.05 (1.38)	29.2 (30.5)	44.5 (46.1)
$f_0(975)$	0^{++}	974.1	0.25	0.05 (0.07)	1.48 (1.58)	2.29 (2.40)
$f_0(1250)$	0^{++}	1250	3.4	0.21 (0.31)	8.38 (8.99)	13.2 (13.9)
$f_2(1270)$	2^{++}	1275	3.19	0.88 (1.32)	36.8 (39.5)	57.8 (61.0)
$a_2(1320)$	2^{++}	1318.2	1.14	0.26 (0.40)	11.6 (12.5)	18.4 (19.4)
$\pi_2(1670)$	2^{-+}	1670	1.41	0.10 (0.16)	6.40 (6.75)	10.2 (10.6)

glueballs: MIT bag model, potential models, QCD sum rules, lattice gauge theory, flux-tube model, method of vacuum correlators. For a review of the theoretical models we refer to [33]; the method of vacuum correlators is presented in [34]. One problem of searching for evidence is the possible mixture between gluonic and quarkonic states. The existence of exotic quantum number combinations J^{PC}, which are kinematically forbidden for $q\bar{q}$ states such as 0^{--}, 0^{+-}, and 1^{-+}, would be direct evidence for glueballs. The electromagnetic production of glueballs should also be studied, because this could contribute a strong background to a possible signal for a quark-gluon plasma.

We consider here the two glueball candidates $\eta(1440)$ with mass $m = 1440$ MeV and quantum number J^{PC} 0^{-+} and $f_2(1720)$ with mass $m = 1713$ MeV and quantum number 2^{++} [27], which eventually mix with other mesons. Again the physical important input for the electromagnetic production is the two-photon decay width, which in the framework of the above-mentioned QCD models has been evaluated. Several groups worked out the two-photon decay width of $\eta(1440)$ to be 4.3 keV [35], 2.5 keV [36,37], 15.9 keV [38], and 3.7 keV [39]. From experimental data one can deduce an upper limit of 3.2 keV [33]. The two-photon decay width of the most promising glueball candidate $f_2(1720)$ is predicted to lie in the range of keV [33], whereas the experimental limits are below approximately 0.3 keV [40,33]. For further discussion we will vary the two-photon decay widths of the two candidates from 0.1 keV to 10 keV.

In Fig. 7 we show the calculated Weizsäcker-Williams cross sections of the two candidates in dependence on their two-photon decay widths $\Gamma_{X\to\gamma\gamma}$ for the three collider: SSC ($\gamma = 8000$), which yields the largest cross sections, LHC ($\gamma = 3500$), and RHIC ($\gamma = 100$). According to Fig. 6 the reduced cross sections will only be by about 5–10% smaller than the Weizsäcker-Williams cross sections for SSC and LHC energies; for RHIC energies the reduction amounts to about 40%. In general the production cross sections for the glueball candidates are expected to be in between 0.01 mb and 100 mb. With a RHIC luminosity of 10^{26} cm^{-2} sec^{-1} and a running time of 10^7 sec about 10^5 glueball mesons per year could be produced ($\Gamma_{\gamma\gamma} = 1$ keV); at LHC and SSC about 10^8 – 10^9 glueball mesons could be produced per year assuming a luminosity of 10^{28} cm^{-2} sec^{-1}.

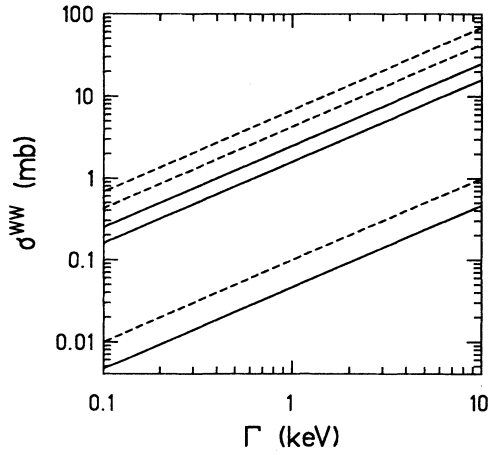

FIG. 7. Weizsäcker-Williams cross section for the production of the two glueball candidates $\eta(1440)$ (solid lines) and $f_2(1720)$ (dashed lines) in a Pb+Pb collision in dependence on the two-photon decay width for SSC, LHC, and RHIC energies.

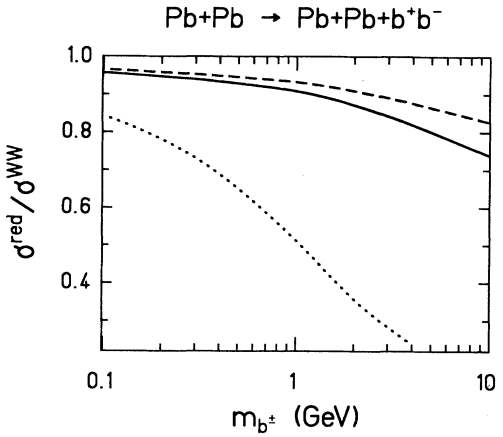

FIG. 8. Reduction factors σ^{red}/σ^{WW} in dependence on the charged boson mass for RHIC ($\gamma = 100$, dotted line), LHC ($\gamma = 3500$, solid line), and SSC ($\gamma = 8000$, dashed line) energies in a Pb+Pb collision.

C. Charged mesons

As for the neutral scalar and pseudoscalar mesons considered before, the electromagnetic production of a pair of charged mesons in an ultrarelativistic heavy-ion collision would allow one to study their properties as, for example, electromagnetic form factors, decay modes, and

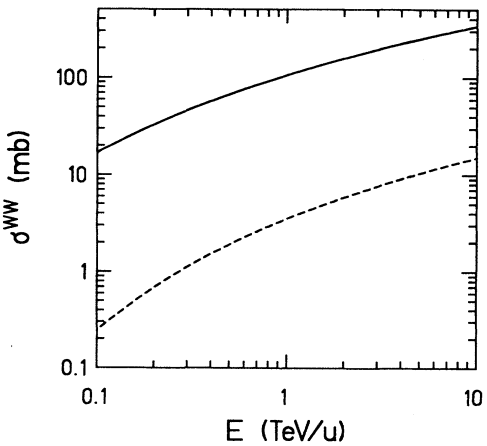

FIG. 9. Weizsäcker-Williams cross section for $\pi^\pm$ (solid line) and $K^\pm$ (dashed line) production in a Pb+Pb collision in dependence on the energy per nucleon.

TABLE II. Cross sections of various charged mesons.

		σ^{red} (σ^{WW}) (mb)		
Particle	Mass (MeV)	$\gamma = 100$	$\gamma = 3500$	$\gamma = 8000$
$\pi^{\pm}$	139.57	12.8 (15.6)	194 (204)	289 (300)
$K^{\pm}$	493.65	0.14 (0.22)	7.54 (8.11)	12.3 (13.0)
$D^{\pm}$	1869	0.18 (0.48) $\times 10^{-3}$	0.19 (0.22)	0.37 (0.41)
$D_s^{\pm}$	1968.8	0.13 (0.36) $\times 10^{-3}$	0.17 (0.19)	0.32 (0.35)
$B^{\pm}$	5278.6	0.03 (0.15) $\times 10^{-6}$	8.12 (10.0) $\times 10^{-3}$	19.8 (22.8) $\times 10^{-3}$

decay widths. However, in our calculations we will assume the charged mesons to be pointlike. In addition, final state interactions are neglected. As a consequence the computed results are expected to slightly overpredict the realistic cross sections.

Figure 8 displays the reduction factors $\sigma^{\mathrm{red}}/\sigma^{\mathrm{WW}}$ for the charged meson production in Pb+Pb collisions in dependence on the charged boson mass for various collider energies. As for the neutral mesons considered before, the reduction factors stay very close to one for LHC and SSC energies for the considered masses, so that the reduced cross sections are nearly equal to the Weizsäcker-Williams cross sections. For RHIC energies the situation is different, because of the reasons discussed above.

In Figs. 9 and 10 we plot the total equivalent photon cross section σ^{WW} for the production of several charged boson pairs in a Pb+Pb collision. We summarize the reduced production cross sections of various charged mesons in Table II.

V. ELECTROMAGNETIC PRODUCTION OF LEPTONS

With respect to a possible diagnostic of the quark-gluon plasma formation the electromagnetic production of dileptons has to be distingushed from hadronic processes for dilepton production. The two-photon production mechanism of lepton pairs can become an important background to lepton measurements, also discussed in [41,42]. Since electron-positron pair production violates the unitarity of the S-matrix element and therefore perturbation theory breaks down in the relativistic energy region, we restrict our consideration on the production of $\mu^{\pm}$ and $\tau^{\pm}$. The Weizsäcker-Williams cross sections for $e^{\pm}$ production yield too high results, but a reinterpretation of the impact-parameter dependent cross section into pair creation multiplicities offers the possibility of measuring the impact parameter [43]. Again we will restrict our considerations to the electromagnetic production without interaction between the produced leptons and between leptons and nuclei.

In Fig. 11 we show the total equivalent photon cross section of $\mu^{\pm}$ production in a Pb+Pb collision. Because of the considered energy range and the low mass of the muon, $m_{\mu} = 105.66$ MeV, the reduction of the total cross section due to the disregarding of the central collision region causes almost no modification. For RHIC energies ($E = 100$ GeV/nucleon) the total cross section is $\sigma^{\mathrm{WW}} = 0.24$ b, for LHC energies ($E = 3.5$ TeV/nucleon) we computed $\sigma^{\mathrm{WW}} = 2.7$ b, and for SSC energies ($E = 8$

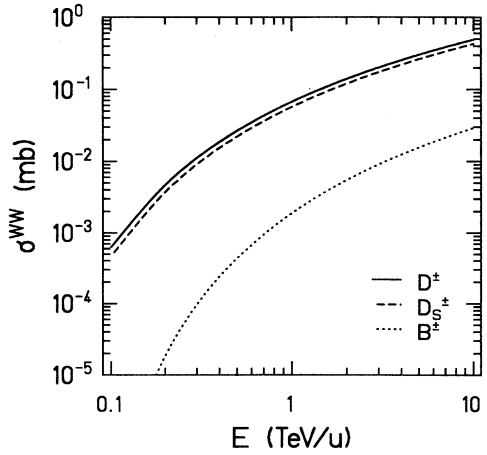

FIG. 10. Weizsäcker-Williams cross section for $D^{\pm}$ (solid line), $D_s^{\pm}$ (dashed line), and $B^{\pm}$ (dotted line) production in a Pb+Pb collision in dependence on the energy per nucleon.

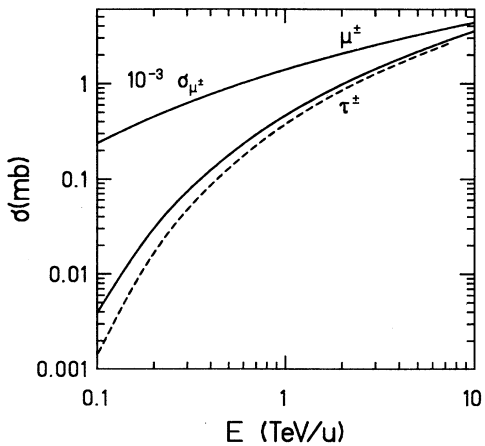

FIG. 11. Weizsäcker-Williams cross section for $\mu^{\pm}$ production (top solid) as well as Weizsäcker-Williams (solid) and reduced (dashed) cross section for $\tau^{\pm}$ production in a Pb+Pb collision in dependence on the energy per nucleon. The total cross section for muon production ranges between $\sigma_{\mu^{\pm}} = 0.24$ b for $E = 0.1$ TeV/nucleon and $\sigma_{\mu^{\pm}} = 4.4$ b for $E = 10$ TeV/nucleon.

TeV/nucleon) we found $\sigma^{WW} = 4.0$ b. In the case of $\tau^{\pm}$ production the reduction can be somewhat more significant, since the mass of $\tau^{\pm}$ is $m_\tau = 1784.1$ MeV. The total cross section (solid line) for $\tau^{\pm}$ production is also displayed in Fig. 11, where the reduced cross section is represented by the dashed line. For RHIC energies ($\gamma = 100$) the total cross section is $\sigma^{WW} = 2.9$ μb, whereas the reduced cross section is $\sigma^{red} = 1.0$ μb. For LHC energies ($\gamma = 3500$) we computed $\sigma^{WW} = 1.55$ mb and $\sigma^{red} = 1.38$ mb, and for SSC energies ($\gamma = 8000$) we obtained $\sigma^{WW} = 2.92$ mb and $\sigma^{red} = 2.70$ mb.

VI. CONCLUSIONS

We have discussed the electromagnetic production of various exotic particles in ultrarelativistic heavy-ion collisions. The electromagnetic production of intermediate mass Higgs bosons of the minimal supersymmetric extension of the standard model may be enhanced over the standard model Higgs boson production. For certain choices of the free model parameters the enhancement may well be a factor of about 10; of course, other choices exist, where the enhancement turns into a suppression. Assuming the optimistic cases to hold in nature, it turns out that for the expected luminosities of the two ultrarelativistic heavy-ion colliders LHC and SSC the production rates of the intermediate mass MSSM Higgs bosons are still too small to be safely detectable by their rare decay modes, which are the two-photon decay and the four-lepton decay. Contrary to that, the main decay mode, i.e., the decay into a $b\bar{b}$ quark pair, might yield clear detection signals; as the number of the $b\bar{b}$ signal decays increases with the enhanced production of the intermediate MSSM Higgs bosons with respect to the SM Higgs boson case, the background of directly produced $b\bar{b}$ pairs remains unaffected. As a consequence the MSSM Higgs bosons might be detectable as a small peak in the invariant $b\bar{b}$-mass spectrum; of course, a full acceptance detector would be necessary and eventually also cuts in the $p_\perp$ spectrum. Here it would be extremely important to know the rapidity and tranverse momentum distribution of the Higgs bosons, which are not necessarily produced at rest. Similiar conclusions hold for the electromagnetic production of supersymmetric particles. After discarding the central impact-parameter region in the production cross section, still about a few hundred of not too heavy supersymmetric particles could be produced at LHC or SSC per year. In principle this could be sufficient for their detection. Again a full acceptance detector would be appreciated. Besides the production of such heavy exotic particles as Higgs bosons or supersymmetrical particles, ultrarelativistic heavy-ion collisions could also be used to produce mesons and study their properties. Of considerable importance is the investigation of the two glueball candidates. Electromagnetic production cross sections are well within the mb region, so that production rates are rather high even for RHIC collider energies. We also studied the electromagnetic production of leptons, which also contribute to the background for leptonic signals of a quark-gluon plasma formation.

ACKNOWLEDGMENTS

One of us (M. G.) wants to thank the Alexander von Humboldt Stiftung for its support with the Feodor Lynen Foundation. We also would like to thank Tom Weiler for bringing the Higgs bosons of the minimal supersymmetric extension of the standard model to our attention and for helping us to clarify some of the mystique about the loop amplitudes in the corresponding two-photon decay widths.

[1] M. Greiner, D. Hilberg, C. Hofmann, and G. Soff, J. Phys. G **19**, 261 (1993).
[2] M. Vidović, M. Greiner, C. Best, and G. Soff, Phys. Rev. C **47**, 2308 (1993), this issue.
[3] M. Grabiak, B. Müller, W. Greiner, G. Soff, and P. Koch, J. Phys. G **15**, L25 (1989).
[4] E. Papageorgiu, Phys. Rev. D **40**, 92 (1989).
[5] E. Papageorgiu, Phys. Lett. B **250**, 155 (1990).
[6] M. Drees, J. Ellis, and D. Zeppenfeld, Phys. Lett. B **223**, 454 (1989).
[7] R. N. Cahn and J. D. Jackson, Phys. Rev. D **42**, 3690 (1990).
[8] G. Baur and L. Ferreira Filho, Nucl. Phys. **A518**, 786 (1990).
[9] J. S. Wu, C. Bottcher, M. R. Strayer, and A. K. Kerman, Ann. Phys. **210**, 402 (1991).
[10] B. Müller and A. J. Schramm, Phys. Rev. D **42**, 3699 (1990).
[11] J. W. Norbury, Phys. Rev. D **42**, 3696 (1990).
[12] K. J. Abraham, R. Laterveer, J. A. M. Vermaseren, and D. Zeppenfeld, Phys. Lett. B **251**, 186 (1990).
[13] M. Greiner, M. Vidović, J. Rau, and G. Soff, J. Phys. G **17**, L45 (1991).
[14] K. J. Abraham, M. Drees, R. Laterveer, E. Papageorgiu, A. Schäfer, G. Soff, J. Vermaseren, and D. Zeppenfeld, in Proceedings of the Coherent Processes in Heavy-Ion Collisions at the LHC, Large Hadron Collider Workshop, Aachen, 1990, edited by G. Jarlskog and D. Rein (CERN Report No. CERN 90-10, ECFA 90-133, 1990), Vol. II, p. 1224.
[15] T. D. Lee, *Particle Physics and Introduction to Field Theory* (Harwood Academic, Chur, 1981).
[16] J. F. Gunion, H. Haber, G. Kane, and S. Dawson, *The Higgs Hunter's Guide* (Addison-Wesley, Reading, 1991).
[17] Y. Okada, M. Yamaguchi, and T. Yamagido, Prog. Theor. Phys. **85**, 1 (1991).
[18] H. Haber and R. Hempfling, Phys. Rev. Lett. **66**, 1815 (1991).
[19] J. Ellis, G. Ridolfi, and F. Zwirner, Phys. Lett. B **257**, 83 (1991).

[20] P. H. Chankowski, S. Pokorski, and J. Rosiek, Phys. Lett. B **274**, 191 (1992).
[21] D. M. Pierce, A. Papadopoulos, and S. B. Johnson, Phys. Rev. Lett. **68**, 3678 (1992).
[22] V. Barger, M. S. Berger, A. L. Stange, and R. J. N. Phillips, Phys. Rev. D **45**, 4128 (1992).
[23] T. J. Weiler and T. C. Yuan, Nucl. Phys. **B318**, 337 (1989); confer also J. F. Gunion and H. Haber, *ibid.* **B272**, 1 (1986).
[24] A. Bartl, H. Fraas, and W. Majerotto, Z. Phys. C **30**, 441 (1986).
[25] G. Soff, J. Rau, M. Grabiak, B. Müller, and W. Greiner, in *The Nuclear Equation of State*, edited by W. Greiner and H. Stöcker (Plenum, New York, 1989), Part B, p. 579.
[26] K. Hidaka, Y. Kizukuri, and T. Kon, Phys. Lett. B **278**, 155 (1992), and references therein.
[27] Particle Data Group, Phys. Lett. B **239**, 1 (1990); Phys. Rev. D **45**, 2 (1992).
[28] J. F. Gunion, G. Gamberini, and S. F. Novaes, Phys. Rev. D **38**, 3481 (1988).
[29] J. Rau, B. Müller, W. Greiner, and G. Soff, J. Phys. G **16**, 211 (1990).
[30] K. Karch, DESY Report No. DESY 91-094, ISSN 0418-9833, 1991.
[31] S. E. Baru *et al.*, Z. Phys. C **48**, 581 (1990).
[32] K. Karch *et al.*, Z. Phys. C **54**, 33 (1992).
[33] F. Close, Rep. Prog. Phys. **51**, 833 (1988).
[34] H. G. Dosch and Yu. A. Simonov, Z. Phys. C **45**, 147 (1989).
[35] F. Caruso, E. Predazzi, A. C. B. Antunes, and J. Tiomno, Z. Phys. C **30**, 493 (1986).
[36] M. Frank and P. J. O'Donnel, Phys. Rev. D **32**, 1739 (1985).
[37] N. N. Achasov and G. N. Shestakov, Phys. Lett. B **156**, 434 (1985).
[38] H. E. Haber and J. P. Perrier, Phys. Rev. D **32**, 2961 (1985).
[39] K. Geiger, B. Müller, and W. Greiner, Z. Phys. C **48**, 257 (1990).
[40] L. Köpke and N. Wermes, Phys. Rep. **174**, 67 (1989).
[41] C. Bottcher and M. R. Strayer, Phys. Rev. D **39**, 1330 (1989).
[42] G. Baur, Z. Phys. C **54**, 419 (1992).
[43] C. Best, W. Greiner, and G. Soff, Phys. Rev. A **46**, 261 (1992).